

Nonlinear temporal dynamics of a strongly coupled quantum-dot–cavity system

Arka Majumdar,^{1,*} Dirk Englund,² Michal Bajcsy,¹ and Jelena Vučković¹¹*E. L. Ginzton Laboratory, Stanford University, Stanford, California 94305, USA*²*Department of Electrical Engineering and Department of Applied Physics, Columbia University, New York, New York 10027, USA*

(Received 19 October 2011; published 5 March 2012)

We theoretically analyze the temporal dynamics of strongly coupled quantum-dot–cavity system driven by a resonant laser pulse and observe the signature of Rabi oscillation in the time-resolved response of the system (i.e., in the numerically calculated cavity output). We derive simplified linear and nonlinear semiclassical models that approximate well the system’s behavior in the limits of high- and low-power driving pulses and describe the role of quantum coherence in the exact dynamics of the system. Finally, we also present time-resolved transmission measurements showing the dynamics of a quantum-dot–cavity system in the presence of a short laser pulse.

DOI: [10.1103/PhysRevA.85.033802](https://doi.org/10.1103/PhysRevA.85.033802)

PACS number(s): 42.50.Pq, 78.67.Hc, 78.67.De, 85.35.Be

I. INTRODUCTION

A single quantum dot (QD) coupled to a photonic crystal microcavity constitutes an integrated nanophotonic platform for probing solid-state cavity quantum electrodynamic (CQED) effects [1]. The eigenstates of this coupled system form an anharmonic ladder, which results in an optical nonlinearity at a single photon level. In recent years, this nonlinearity has been used to perform all-optical [2,3] and electro-optic switching [4] as well as to generate nonclassical states of photons [5–7].

In this paper, we study the temporal dynamics of the coupled dot-cavity system driven by a short laser pulse [Fig. 1(a)] using a full quantum optical numerical simulation. The oscillatory behavior of the cavity output [Fig. 1(b)], which is caused by the vacuum Rabi splitting, is analyzed at low, intermediate, and high intensity of the driving laser. Specifically, we derive a linear semiclassical description of the system (similar to Refs. [8,9]) and show that under weak driving, the coupled QD-cavity system follows the same dynamics as a set of two classical linear coupled oscillators. Following this, we describe an improved, nonlinear semiclassical model that mimics the quantum optical model very well for both very low and high peak intensity of the driving pulse. However, the nonlinear semiclassical model deviates from the quantum optical description at intermediate peak intensities of the drive pulse, and we show that this discrepancy arises from the coherence present in the quantum optical system. Finally, we present a study of the temporal dynamics as a function of the major parameters describing the cavity-QD system as well as experimental data showing the signature of the Rabi oscillation in the time domain and the dependence of these oscillations with laser power signifying the nonlinear nature of the system. We note that temporal Rabi oscillations were previously reported in atomic CQED system with a single atom [10] but not with a single solid-state quantum emitter. In the solid-state system, much larger dipole-cavity interaction strength is possible due to the large QD dipole moment and tight confinement of the light field inside the small mode-volume cavity (the vacuum Rabi frequency is on the order of ~ 10 GHz compared to MHz in atomic

CQED systems) [11,12]. As a result, the temporal dynamics probed here is much faster than that previously reported in the atomic system [10]. We note that time-resolved Rabi oscillations were previously analyzed theoretically [13] and experimentally [14] with quantum well excitons embedded in planar microcavities. However, that system is very different from a single quantum emitter (e.g., single quantum dot) embedded in a nanocavity, which we study in this paper and in which time-resolved vacuum Rabi oscillation has not been studied previously. Moreover, we study nonlinear dynamics and power dependence of Rabi oscillations, which have not been studied in other systems [13,14].

II. QUANTUM AND SEMICLASSICAL DESCRIPTION

In the rotating-wave approximation, the quantum-mechanical Hamiltonian \mathcal{H} describing the coherent dynamics of the coupled QD-cavity system is given by [15]

$$\mathcal{H} = \omega_a \sigma^\dagger \sigma + \omega_c a^\dagger a + ig(a\sigma^\dagger - a^\dagger \sigma). \quad (1)$$

Here, ω_c and ω_a are, respectively, the resonance frequencies of the cavity and the QD; a is the annihilation operator for the cavity mode; $\sigma = |g\rangle\langle e|$ is the lowering operator for the QD with excited state $|e\rangle$ and ground state $|g\rangle$; g is the coherent interaction strength between the QD and the cavity, and \hbar is set to 1. When this system is coherently driven by a laser pulse with an electric-field amplitude envelope $\Omega(t) = \Omega_0 p(t)$ and a center frequency ω_l , the driven Hamiltonian in a frame rotating at the frequency ω_l is

$$H = \Delta_c a^\dagger a + \Delta_a \sigma^\dagger \sigma + ig(a^\dagger \sigma - a \sigma^\dagger) + i\Omega(t)(a - a^\dagger). \quad (2)$$

Here, Δ_c and Δ_a are the detuning of the cavity and the QD resonance from the laser frequency; Ω_0 is the maximum laser strength, and $p(t)$ is proportional to the envelope of the laser electric field. Also taking into account the dissipation of the cavity field to the environment with a decay rate κ and a dipole spontaneous emission rate γ , the dynamics of the QD-cavity system are determined by the master equation

$$\frac{d\rho}{dt} = -i[H, \rho] + 2\kappa \mathcal{L}[a] + 2\gamma \mathcal{L}[\sigma], \quad (3)$$

*arkam@stanford.edu

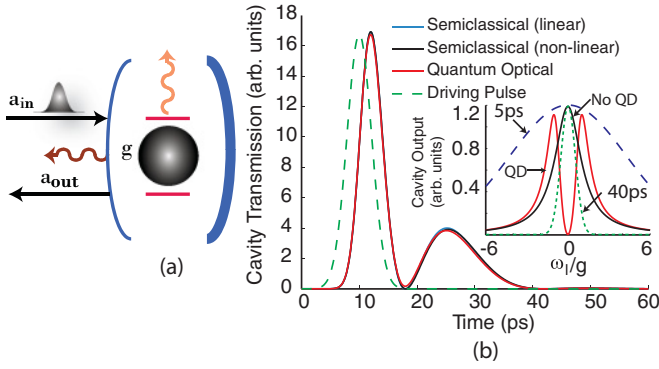


FIG. 1. (Color online) (a) The schematic of the coupled QD-cavity system. It is driven by a laser pulse, and the cavity output is monitored. (b) The cavity transmission calculated by three different models: the quantum optical (red), semiclassical linear (blue) and nonlinear (black) model at low ($\Omega_0/2\pi = 1$ GHz) peak intensity of the driving pulse. All three models match quite well. The input pulse is also shown (green dashed line). The oscillation in the cavity output is due to Rabi oscillation of the photon between the QD and the cavity. The inset shows the cavity transmission spectrum in the presence and in the absence of the strongly coupled QD. The split resonances are separated approximately by twice the coherent dot-cavity interaction strength g . The spectral shape of laser pulses with pulse lengths of 5 ps (blue dashed line) and 40 ps (green dashed line) is also shown. Parameters used for the simulations are $g/2\pi = 25$ GHz, $\kappa/2\pi = 29$ GHz, and $\gamma/2\pi = 1$ GHz.

where ρ is the density matrix of the coupled QD-cavity system. $\mathcal{L}[D]$ is the Lindblad operator corresponding to a collapse operator D to model the incoherent decays and is given by

$$\mathcal{L}[D] = D\rho D^\dagger - \frac{1}{2}D^\dagger D\rho - \frac{1}{2}\rho D^\dagger D. \quad (4)$$

The master equation is solved using numerical integration routines provided in the quantum optics toolbox, truncating the photon states to 20 photons [16]. This method is completely quantum mechanical, and no approximation (other than the standard Born-Markov approximation and truncation of Fock state basis) is made.

A semiclassical description of the coupled system [17] can be derived by using the relation

$$\frac{d\langle D \rangle}{dt} = \text{Tr} \left[D \frac{d\rho}{dt} \right], \quad (5)$$

which is valid for any operator D . The mean-field dynamical equations for the coupled QD-cavity system can then be written as

$$\frac{d\langle a \rangle}{dt} = -\kappa \langle a \rangle + g \langle \sigma \rangle - \sqrt{\kappa} \Omega(t), \quad (6)$$

$$\frac{d\langle \sigma \rangle}{dt} = -\gamma \langle \sigma \rangle + g \langle a \sigma_z \rangle, \quad (7)$$

$$\frac{d\langle \sigma_z \rangle}{dt} = -2\gamma \langle \sigma_z \rangle + 1 - 2g(\langle a^\dagger \sigma \rangle + \langle a \sigma^\dagger \rangle), \quad (8)$$

where $\sigma_z = |e\rangle\langle e| - |g\rangle\langle g|$. We note that this set of equations is not complete; for an exact solution we need to find the equations describing all the other higher-order moments, namely, $\langle a \sigma_z \rangle$ and $\langle a \sigma^\dagger \rangle$. However, in the low-excitation regime (no more than one photon in the system), the QD will

remain mostly in its ground state, and we can approximate $\langle \sigma_z \rangle \approx -1$ and replace $\langle a \sigma_z \rangle = -\langle a \rangle$. The resulting set of equations

$$\frac{d\langle a \rangle}{dt} = -\kappa \langle a \rangle + g \langle \sigma \rangle - \sqrt{\kappa} \Omega(t), \quad (9)$$

$$\frac{d\langle \sigma \rangle}{dt} = -\gamma \langle \sigma \rangle - g \langle a \rangle \quad (10)$$

is identical to the set of equations describing the dynamics of two coupled linear classical oscillators (see Appendix A). Although this approximation neglects the nonlinear nature of the QD, it matches the actual output quantitatively at low excitation power. However, with increasing drive intensities Ω_0 , this model fails completely, as the approximation $\langle \sigma_z \rangle \approx -1$ becomes invalid. For sufficiently high drive intensities, however, one can approximate $\langle \sigma_z \rangle \rightarrow 0$, and Eq. (7) simplifies to

$$\frac{d\langle \sigma \rangle}{dt} = -\gamma \langle \sigma \rangle. \quad (11)$$

Alternatively, we can retain the dynamics of the σ_z term, while making the set of Eqs. (6)–(8) complete by using the approximations $\langle a \sigma_z \rangle \approx \langle a \rangle \langle \sigma_z \rangle$ and $\langle a^\dagger \sigma \rangle \approx \langle a^\dagger \rangle \langle \sigma \rangle$ [9]. While this approach neglects the coherence of the system while analyzing the mean-field dynamical equations, the nonlinear behavior of the QD is taken into account.

Figure 1(b) compares the time-resolved cavity transmission in the low-excitation limit ($\Omega_0/2\pi = 1$) when calculated by the three different models: (i) semiclassical in the linear approximation, (ii) semiclassical in the nonlinear approximation, and (iii) the numerical master equation solution up to truncated Fock state basis $n = 15$. For the numerical simulation, we used a Gaussian pulse with full width at half maximum (FWHM) of 5 ps to drive the dot-cavity system with a pulse with bandwidth higher than the coupled system [as shown in the inset of Fig. 1(b)]. In this low-excitation limit, all three models closely agree and exhibit an oscillation in the cavity transmission. This oscillation is due to the coherent Rabi oscillation of the photons between the QD and the cavity and vanish when $g \rightarrow 0$. Note that further oscillations are quenched by the decay of the cavity field.

To intuitively understand the origin of the oscillation, one can consider the analytical solution of the linear semiclassical equations to find the eigenvalues of the lossy coupled system:

$$\omega_{\pm} = \frac{\omega_c + \omega_d}{2} - i \frac{\kappa + \gamma}{2} \pm \sqrt{g^2 + \frac{1}{4}[\delta - i(\kappa - \gamma)]^2}, \quad (12)$$

where $\delta = \Delta_c - \Delta_a$ is the dot-cavity detuning. In the dot-cavity system the dipole spontaneous emission rate γ is very small. Hence, when $g > \kappa/2$, the system is in the strong-coupling regime, and the split resonance appearing in the cavity transmission spectrum [inset of Fig. 1(b)] will be the result of the formation two distinct energy eigenstates in the system. At the same time without a coupled QD, a single Lorentzian peak is observed in the spectrum of the cavity transmission. The two peaks then correspond to the entangled states of the QD and the cavity, known as polaritons. When the cavity is driven with a short pulse with bandwidth larger than that of the coupled system, the cavity output is

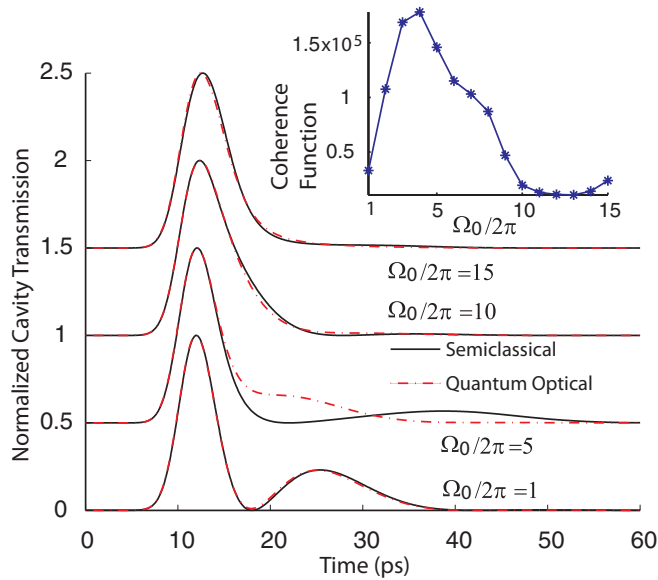


FIG. 2. (Color online) Comparison between the temporal cavity transmission obtained via the quantum optical (red dashed line) and the semiclassical nonlinear (black solid line) models. The cavity transmission is normalized by the maximum cavity transmission, and plots are vertically offset for clarity. The two models match quite well at low and high driving power, but at intermediate power, they differ. The inset shows the coherence, calculated as $(\langle a^\dagger \sigma \rangle - \langle a^\dagger \rangle \langle \sigma \rangle) / \Omega_0^2$, integrated over time as a function of the driving strength Ω_0 . We observe that quantity increases in the intermediate driving power. Parameters used for the simulations are $g/2\pi = 25$ GHz and $\kappa/2\pi = 29$ GHz.

modulated at the frequency difference between the polaritons, i.e., $2\sqrt{g^2 + \frac{1}{4}[\delta - i(\kappa - \gamma)]^2}$.

Although the nonlinear semiclassical model allows QD saturation, it neglects the quantum-mechanical coherence between the QD and the cavity. Figure 2 compares the semiclassical and quantum optical simulations of the coupled dot-cavity system. We find that the results match well both at low (when the QD excited-state population is almost zero and $\langle \sigma_z \rangle \sim -1$) and high (when the QD is saturated and $\langle \sigma_z \rangle \sim 0$) intensities of the driving field. As expected, the nonlinear semiclassical approach deviates for intermediate intensities. As a measure of the coherence, we plot the quantity $C = (\langle a^\dagger \sigma \rangle - \langle a^\dagger \rangle \langle \sigma \rangle) / \Omega_0^2$ integrated over time as a function of the driving strength Ω_0 in the inset of Fig. 2. C is zero in the absence of any coherence and is much smaller for low and high excitation powers than in the intermediate-excitation regime. Note that the onset of the increase in the higher excitation power is due to numerical errors caused by the truncated Fock state basis.

III. DEPENDENCE ON THE SYSTEM PARAMETERS

We are now in a position to characterize the temporal cavity transmission as a function of four relevant parameters describing the coupled dot-cavity system: dot-cavity detuning δ , the dot-cavity coupling rate g , the cavity field decay rate κ , and pure QD dephasing rate γ_d . Figure 3(a) shows that the time interval between two peaks decreases as the QD-cavity

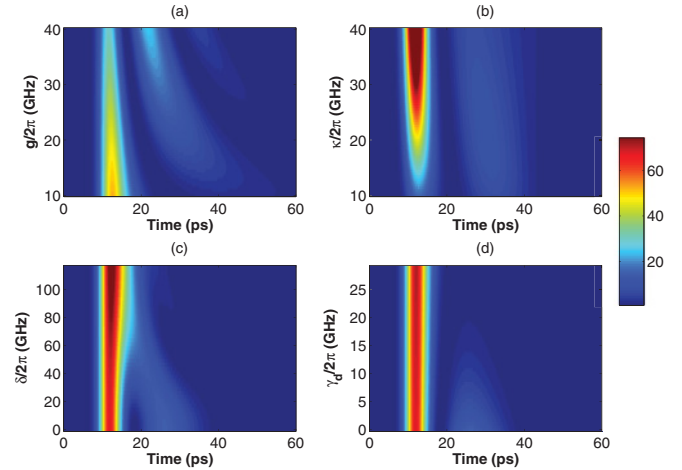


FIG. 3. (Color online) The temporal cavity output obtained from the full quantum optical simulation as a function of (a) the dot-cavity coupling strength g (here $\kappa/2\pi = 20$ GHz; $\delta = 0$ and $\gamma_d = 0$), (b) the cavity field decay rate κ (here $g/2\pi = 20$ GHz; $\delta = 0$ and $\gamma_d = 0$), (c) the dot cavity detuning δ (here $g/2\pi = \kappa/2\pi = 20$ GHz and $\gamma_d = 0$), and (d) the pure QD dephasing rate γ_d (here $g/2\pi = \kappa/2\pi = 20$ GHz and $\delta = 0$). For all the simulations a low excitation power ($\Omega_0/2\pi = 2$) is assumed.

coupling rate g increases. This observation is consistent with the oscillation period as predicted by the simple linear analysis. At the same time, the oscillation period depends only weakly on κ [Fig. 3(b)]. We note an increasing cavity output with increasing cavity decay rate κ , which is due to the increasing overlap between the input pulse and the cavity spectrum. The oscillation frequency increases with increasing detuning between the dot and the cavity; when the QD is detuned too far from the cavity, the oscillation almost disappears. This is expected, as with large enough detuning, the input pulse is

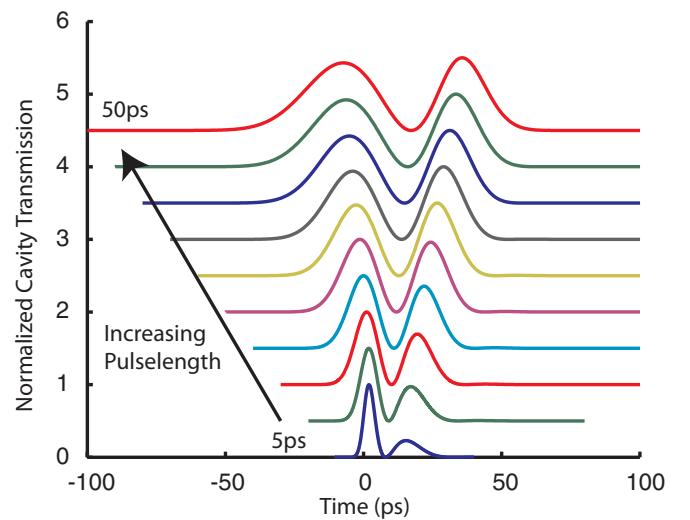


FIG. 4. (Color online) The normalized cavity transmission for different pulse durations. The pulse duration is changed from 5 to 50 ps. We observe oscillation in the cavity output, although the oscillation frequency decreases with increasing pulse width. This can be explained by the reduced overlap between the pulse and the coupled dot-cavity system in frequency domain.

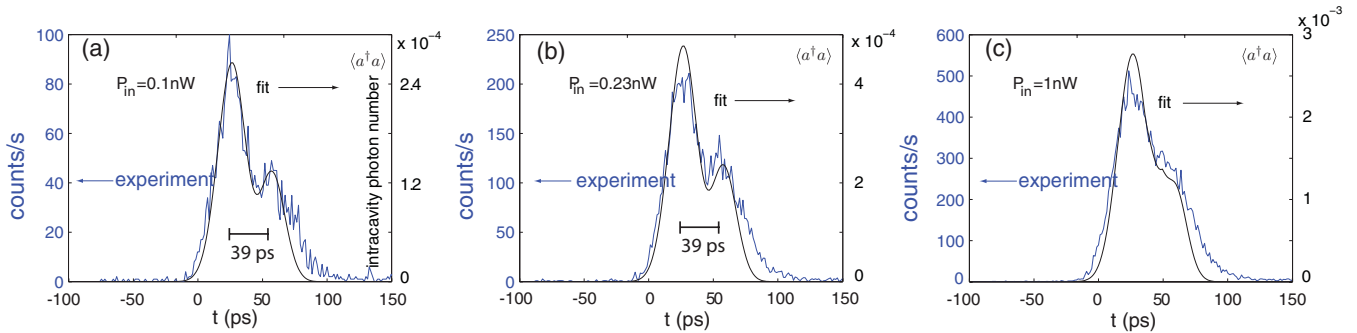


FIG. 5. (Color online) Experimentally measured time-resolved transmission of 40-ps pulses through a strongly coupled dot-cavity system for three different powers (averaged over the pulse repetition period): (a) 0.1 nW, (b) 0.23 nW, and (c) 1 nW. The powers are measured in front of the objective lens in the confocal microscopy setup. For this specific system cavity field decay rate $\kappa/2\pi = 29$ GHz, and coherent dot-cavity coupling strength $g/2\pi = 25$ GHz. Clear oscillations are observed in the cavity transmission, consistent with the theoretical predictions. We also observe decreasing oscillation with increasing laser power due to QD saturation.

not affected by the QD [Fig. 3(c)]. An important effect in solid-state cavity QED is pure QD dephasing, which destroys the coherence of the system without affecting the population of the quantum-dot states. The effect of pure QD dephasing can be incorporated by adding the term $2\gamma_d \mathcal{L}(\sigma^\dagger \sigma)$ in the master equation [11,18], where γ_d is the pure QD dephasing rate. Figure 3(d) plots the cavity output as a function of the pure QD dephasing rate γ_d , indicating that the oscillation eventually disappears when the dephasing rate is large.

Finally, we analyze the dependence of the cavity transmission on the pulse duration (Fig. 4). When the pulse duration is changed from 5 to 50 ps, we observe a decreasing oscillation frequency. This can be explained by the reduced overlap between the input pulse and the coupled dot-cavity system with reduction in pulse bandwidth. In other words, a long pulse does not have sufficient bandwidth to excite both the polaritons [as shown in the inset of Fig. 1(b)], and the oscillation frequency in the cavity output deviates more from $2g$.

IV. EXPERIMENTAL DATA

To test the validity of our numerical simulations, we experimentally probed a strongly coupled QD-cavity system. A cross-polarized reflectivity setup was used to obtain the transmission of light through the coupled system, and the cavity transmission was monitored with a Hamamatsu streak camera. Details of the fabrication and the experimental setup can be found in Ref. [12], with the experimental parameters of the probed dot-cavity system being $g/2\pi = 25$ GHz and $\kappa/2\pi = 29$ GHz [2]. We did not observe the predicted oscillations in the initial experiments measuring the transmission of 5-ps pulses through the cavity, most likely because of the limited time resolution of our detector. Subsequently, the experiment was performed with a longer pulse (40-ps FWHM). A long pulse does not have sufficient bandwidth to excite both the polaritons [as shown in the inset of Fig. 1(b)], and the oscillation frequency in the cavity transmission is different from the value $2g$, as shown in Fig. 4. Figures 5(a), 5(b), and 5(c) show the experimentally obtained cavity output for three different excitation powers. The experimental data match qualitatively the predictions from the numerical simulation,

and clear oscillation is observed in the cavity output. This oscillation disappears with increasing laser power, as expected from the QD saturation. The oscillation period is estimated to be 25 GHz, corresponding to a time difference of 39 ps between the two peaks. We note that the numerically obtained plots in Fig. 4 are calculated with very small excitation power. However, the experiment cannot be performed with such low excitation power as the detected signal is too low. Hence, in the experiment, the coupled system is driven close to the QD saturation, and the oscillations are less visible. Another reason is that the extinction of the cross-polarized cavity transmission measurement is not perfect, so the signal will be detected together with light reflected from the surface of the sample that did not interact with the QD-cavity system. Additionally, possible charging of the QD moves the dot far out of resonance and will blur the predicted oscillatory cavity transmission with the nonoscillating spectrum for $g = 0$.

In summary, we have analyzed the nonlinear temporal dynamics of a strongly coupled QD-cavity system driven by a short laser pulse. We showed that this quantum optical system behaves similarly to two coupled classical linear oscillators when the system is driven with a weak pulse and that a signature of the vacuum Rabi oscillations can be observed in the time-resolved cavity transmission. For a strong excitation pulse these oscillations die down due to saturation of the QD. We provided a semiclassical nonlinear model and showed that in the actual dynamics, the role of quantum coherence is important. Last, we presented experimental evidence of those oscillations in the cavity output.

ACKNOWLEDGMENTS

Financial support was provided by the Office of Naval Research (PECASE award), National Science Foundation, and Army Research Office. A.M. was supported by the SGF (through a Texas Instruments Fellowship). Work was performed in part at the Stanford Nanofabrication Facility of NNIN supported by the National Science Foundation. D.E. acknowledges support by the Sloan research fellowship and by the US Air Force Office of Scientific Research Young Investigator Program, AFOSR Grant No. FA9550-11-1-0014.

APPENDIX: DYNAMICS OF TWO CLASSICAL COUPLED LINEAR OSCILLATORS

The dynamics of two classical coupled oscillators, with resonance frequency ω_0 and decay rates Γ_1 and Γ_2 , are governed by

$$\frac{d^2x_1}{dt^2} + \Gamma_1 \frac{dx_1}{dt} + \omega_0^2 x_1 + G(x_1 - x_2) = \Omega(t)e^{i\omega_0 t} \quad (\text{A1})$$

and

$$\frac{d^2x_2}{dt^2} + \Gamma_2 \frac{dx_2}{dt} + \omega_0^2 x_2 + G(x_2 - x_1) = 0, \quad (\text{A2})$$

where G denotes the coupling strength between the oscillators. One of the oscillators is driven resonantly with driving strength $\Omega(t)$, as the cavity is driven by a laser. We assume a solution of the form $x_1(t) = X_1(t)e^{i\omega_0 t}$ and $x_2(t) = X_2(t)e^{i\omega_0 t}$, where $X_1(t)$ and $X_2(t)$ are slowly varying envelopes of the actual

oscillator outputs. Then we can write

$$\begin{aligned} \frac{dx_1}{dt} &= i\omega_0 X_1 e^{i\omega_0 t} + \left(\frac{dX_1}{dt} e^{i\omega_0 t} \right) \\ \frac{d^2x_1}{dt^2} &= 2i\omega_0 \frac{dX_1}{dt} e^{i\omega_0 t} - \omega_0^2 X_1 e^{i\omega_0 t} + \left(\frac{d^2X_1}{dt^2} e^{i\omega_0 t} \right). \end{aligned}$$

For x_2 we can find similar equations. Using the slowly varying envelope approximation ($\frac{dX_1}{dt} \ll i\omega_0 X_1$ and $\frac{d^2X_1}{dt^2} \ll i\omega_0 \frac{dX_1}{dt}, \omega_0^2 X_1$), we remove the bracketed terms and obtain the following equations for the undriven coupled oscillator system:

$$\frac{dX_1}{dt} = -\left(\frac{\Gamma_1}{2} + \frac{G}{2i\omega_0} \right) X_1 + \frac{G}{2i\omega_0} X_2 + \Omega(t) \quad (\text{A3})$$

and

$$\frac{dX_2}{dt} = -\left(\frac{\Gamma_2}{2} + \frac{G}{2i\omega_0} \right) X_2 + \frac{G}{2i\omega_0} X_1. \quad (\text{A4})$$

-
- [1] A. Faraon, A. Majumdar, D. Englund, E. Kim, M. Bajcsy, and J. Vučković, *New J. Phys.* **13**, 055025 (2011).
- [2] D. Englund, A. Majumdar, M. Bajcsy, A. Faraon, P. Petroff, and J. Vučković, *Phys. Rev. Lett.* **108**, 093604 (2012).
- [3] D. Sridharan, R. Bose, H. Kim, G. S. Solomon, and E. Waks, e-print [arXiv:1107.3751v1](https://arxiv.org/abs/1107.3751v1).
- [4] A. Faraon, A. Majumdar, H. Kim, P. Petroff, and J. Vučković, *Phys. Rev. Lett.* **104**, 047402 (2010).
- [5] A. Faraon, I. Fushman, D. Englund, N. Stoltz, P. Petroff, and J. Vučković, *Nat. Phys.* **450**, 859 (2008).
- [6] A. Majumdar, M. Bajcsy, and J. Vučković, e-print [arXiv:1106.1926](https://arxiv.org/abs/1106.1926).
- [7] A. Reinhard, T. Volz, M. Winger, A. Badolato, K. J. Hennessy, E. L. Hu, and A. Imamoglu, *Nat. Photonics* **6**, 93 (2012).
- [8] P. Domokos, P. Horak, and H. Ritsch, *J. Phys. B* **34**, 187 (2001).
- [9] M. A. Armen and H. Mabuchi, *Phys. Rev. A* **73**, 063801 (2006).
- [10] J. Bochmann, M. Mücke, G. Langfahl-Klabes, C. Erbel, B. Weber, H. P. Specht, D. L. Moehring, and G. Rempe, *Phys. Rev. Lett.* **101**, 223601 (2008).
- [11] D. Englund, A. Majumdar, A. Faraon, M. Toishi, N. Stoltz, P. Petroff, and J. Vučković, *Phys. Rev. Lett.* **104**, 073904 (2010).
- [12] D. Englund *et al.*, *Nature (London)* **450**, 857 (2007).
- [13] V. Savona and C. Weisbuch, *Phys. Rev. B* **54**, 10835 (1996).
- [14] T. B. Norris, J.-K. Rhee, C.-Y. Sung, Y. Arakawa, M. Nishioka, and C. Weisbuch, *Phys. Rev. B* **50**, 14663 (1994).
- [15] C. W. Gardiner and P. Zoller, *Quantum Noise* (Springer, Berlin, 2005).
- [16] S. M. Tan, *J. Opt. B* **1**, 424 (1999).
- [17] A. Majumdar, N. Manquest, A. Faraon, and J. Vučković, *Opt. Express* **18**, 3974 (2010).
- [18] A. Majumdar, E. D. Kim, Y. Gong, M. Bajcsy, and J. Vučković, *Phys. Rev. B* **84**, 085309 (2011).